Hydrogen doping in indium oxide: An *ab initio* study

Sukit Limpijumnong,[1,2,3] Pakpoom Reunchan,[1,2] Anderson Janotti,[1] and Chris G. Van de Walle[1]
[1]*Materials Department, University of California, Santa Barbara, California 93106-5050, USA*
[2]*School of Physics, Suranaree University of Technology and Synchrotron Light Research Institute, Nakhon Ratchasima 30000, Thailand*
[3]*Thailand Center of Excellence in Physics (ThEP Center), Commission on Higher Education, Bangkok 10400, Thailand*
(Received 14 August 2009; revised manuscript received 13 October 2009; published 9 November 2009)

First-principles density-functional theory is employed to investigate the role of hydrogen impurities in In_2O_3. We find that both interstitial hydrogen (H_i) and substitutional hydrogen (H_O) act as shallow donors. Our results support recent experiments by Koida *et al.* [Jpn. J. Appl. Phys. **46**, L685 (2007)], which found hydrogen-doped In_2O_3 to be a good candidate for transparent conducting films.

DOI: 10.1103/PhysRevB.80.193202 PACS number(s): 61.72.−y, 71.55.−i

Indium oxide (In_2O_3) is one of the few transparent materials that can be doped to a very high carrier concentration without significantly degrading their transparencies. The most widely used transparent conductor is tin-doped In_2O_3, known as indium tin oxide (ITO), which is used as a transparent electrode for optoelectronic devices such as solar cells and light emitting diodes. Recently, Koida *et al.*[1] showed that hydrogen-doped In_2O_3 can have mobility exceeding 100 $cm^2/V\,s$ at carrier densities of $\sim 10^{20}$ cm^{-3} and exhibits good transparency even at near-infrared (NIR) wavelengths. Hydrogen-doped In_2O_3 is, therefore, a promising material to replace or improve upon ITO for applications in optoelectronic devices such as solar cells or photodetectors, in particular, when sensitivity in the NIR region is required.

In this Brief Report, we provide a detailed first-principles study of H in In_2O_3. In most semiconductors H_i is amphoteric, acting as a donor in *p*-type samples and as an acceptor in *n*-type samples. If H_i is amphoteric, it can never be the cause of conductivity since it self-compensates. There are exceptions though. For example, H_i was proposed, based on first-principles calculations,[2] to act exclusively as a donor in ZnO, a prediction which was soon confirmed by experiments.[3] Hydrogen is thus one of the causes of unintentional *n*-type conductivity in ZnO. In the present work we find that H_i is also a shallow donor in In_2O_3, and can, therefore, also be the cause of *n*-type conductivity. In addition, H atoms can also occupy substitutional oxygen sites (H_O) and also act exclusively as donors in this configuration. Substitutional hydrogen was recently described in terms of a multicenter bond and found to be stable in a number of oxides and some nitride materials.[4–6] In order to explore the stability of H_O, we also performed calculations for oxygen vacancies (V_O) in In_2O_3. Our findings confirm that hydrogen acts as the source of *n*-type conductivity in In_2O_3.

In_2O_3 has a fairly complicated crystal structure called *bixbyite* [space group $T_h^7(Ia\bar{3})$] with 80 atoms in a conventional cell and 40 atoms in the primitive unit cell. Its large primitive unit cell, compared with conventional semiconductors (two atoms per cell for Si or GaAs), rendered first-principles calculations of this material prohibitively demanding in the past. Only in the last decade have first-principles calculations for In_2O_3 been attempted, starting with a linear muffin tin orbital method with atomic sphere approximations with a small basis set for an unrelaxed experimental structure by Odaka *et al.*,[7] followed by a more advanced full-potential linear muffin-tin-orbital calculation that included volume relaxation by Mryasov and Freeman.[8] Based on their investigation of the band structure, Mryasov and Freeman attributed the coexistence of conductivity and transparency to the unique characteristics of the conduction-band separation in In_2O_3. More recently, Medvedeva[9] used the full-potential linearized augmented plane-wave method and allowed full structural relaxations to calculate the band structures. To date, only a few impurities in In_2O_3 have been studied by first-principles calculations.[8–11]

We perform first-principles calculations using density-functional theory (DFT) within the local-density approximation (LDA), as implemented in the Vienna *ab initio* simulation package.[12] Electron-ion interactions are treated using projector augmented wave potentials.[13] The electron wave functions are described using a plane-wave basis set with an energy cutoff of 400 eV. Since In 4*d* electrons are not fully localized near the core and can play a role in the crystal bonding, they are treated as valence electrons and allowed to relax during the self-consistent calculations. A shifted $2\times2\times2$ *k*-point sampling based on the Monkhorst-Pack scheme[14] is employed for the Brillouin-zone integration. The calculated lattice constant of 10.073 Å is in good agreement with the experimental value of 10.117 Å.[15] The calculated band gap (1.17 eV) is much smaller than the experimental value due to the well-known DFT problem. In the past, the experimental band gap of In_2O_3 was widely believed to be 3.6 eV.[16] Only recently has the actual value of the band gap been established, at 2.67 eV for molecular-beam epitaxy (MBE)-grown samples[17] and a slightly higher value at 2.89 eV for rf magnetron sputtered samples.[18] We can overcome the band-gap underestimation inherent in LDA by performing LDA $+U$ calculations, allowing us to investigate the changes in the transition levels and formation energies as the band gap is increased. This approach has been successfully applied in the study of H in other oxides and nitrides.[4–6,19] To calculate H in various configurations, we follow a supercell approach with a conventional unit cell of 80 atoms as the supercell and the lattice constant fixed at the calculated bulk value (10.073 Å). All atoms are allowed to relax during the calculations. The formation energy of H_i^q ($q=-$, 0, or +) is defined as[20,21]

$$E^f(\mathrm{H}_i^q) = E_{\mathrm{tot}}(\mathrm{H}_i^q) - E_{\mathrm{tot}}(\mathrm{bulk}) - \mu_{\mathrm{H}} + qE_F, \quad (1)$$

where $E_{\mathrm{tot}}(\mathrm{H}_i^q)$ is the total energy of the supercell containing H_i in charge state q, and $E_{\mathrm{tot}}(\mathrm{bulk})$ is the total energy of the perfect crystal in the same supercell. For a charged H_i ($q \neq 0$), electrons are exchanged with a reservoir with energy E_F, the Fermi energy of the system. μ_{H} is the hydrogen chemical potential, i.e., the energy of the reservoir with which H atoms are exchanged. We fixed the value of μ_{H} to half of the calculated energy of a free H_2 molecule. The formation energies of V_{O} and H_{O} are defined as

$$E^f(V_{\mathrm{O}}^q) = E_{\mathrm{tot}}(V_{\mathrm{O}}^q) - E_{\mathrm{tot}}(\mathrm{bulk}) + \mu_{\mathrm{O}} + qE_F, \quad (2)$$

and

$$E^f(\mathrm{H}_{\mathrm{O}}^q) = E_{\mathrm{tot}}(\mathrm{H}_{\mathrm{O}}^q) - E_{\mathrm{tot}}(\mathrm{bulk}) + \mu_{\mathrm{O}} - \mu_{\mathrm{H}} + qE_F, \quad (3)$$

where $E_{\mathrm{tot}}(V_{\mathrm{O}}^q)$ is the total energy of the supercell with one O removed, and $E_{\mathrm{tot}}(\mathrm{H}_{\mathrm{O}}^q)$ is the total energy of the supercell with one H substituted for O. For the purposes of presenting our results we assumed In-rich growth conditions, i.e., μ_{In} is fixed at the energy per atom of In metal, and μ_{O} is fixed at 3.66 eV below the energy of half an O_2 molecule, based on the calculated heat of formation of $\mathrm{In}_2\mathrm{O}_3$ (10.99 eV/f.u.). Values for other growth conditions can easily be obtained by referring back to Eqs. (2) and (3).

By symmetry, $\mathrm{In}_2\mathrm{O}_3$ in the bixbyite structure has two inequivalent In sites ($8b$ and $24d$ in Wyckoff notation) and all oxygen sites are equivalent.[15] A quarter of all In atoms (labeled In1) occupy the $8b$ positions while the remaining three quarters (labeled In2) occupy the $24d$ positions. Both types of In atoms have a sixfold coordination with their O neighbors. The calculated local structures of In1 and In2 atoms are shown in Figs. 1(a) and 1(b), respectively. The local structure of In1 atom is quite symmetrical. All six In-O bonds are equivalent with a bond distance of 0.2% smaller than the average value of all In-O bonds. It has a shear distorted octahedral coordination as shown in Fig. 1(a). If all the bond angles were 90°, the structure would be a perfect octahedron. The In2 configuration is less symmetrical, as shown in Fig. 1(b). For In2, the six In-O bonds can be divided into three groups of two equivalent In-O bonds. The major difference between In1 and In2 is that In1 and its O neighbors form three sets of linear O-In-O bonds whereas no linear O-In-O bonds occur for In2. For the local structure of oxygen, each O atom forms distorted tetrahedral bonds with its neighboring In atoms (one In1 and three In2) as shown in Fig. 1(c). These four In-O bonds are inequivalent and have bond distances that differ from the average bond distance ($d_{\mathrm{In\text{-}O}}^{\mathrm{calc.}}$ =2.169 Å) by +2.0%, +0.5%, −0.2%, and −2.3%.

We have calculated H_i in three charge states: +, neutral, and −. Similar to other oxides[2,22] and nitrides,[20,23] H_i^+ prefers sites near the anions. In other oxides and nitrides, H_i^+ exhibits local minima at the bond center (BC) and anion antibonding (AB_{O}) sites. For $\mathrm{In}_2\mathrm{O}_3$ there are four inequivalent BC and four inequivalent AB_{O} sites, as illustrated in Fig. 1(d). We find that H_i^+ is not stable at the BC sites. It is spontaneously pushed away from the site and moves significantly off-axis (similar to the $\mathrm{OA}_{\parallel}$ site in Ref. 24). Indeed, two of the BC sites lead to configurations that are essentially the same as the $\mathrm{AB}_{\mathrm{O3}}$ and $\mathrm{AB}_{\mathrm{O4}}$ sites. The calculated energies for H_i^+ at the four inequivalent AB_{O} sites are listed in Table I. It has been previously shown for the cases of ZnO (Ref. 2) and III-Nitrides[20,23] that when H occupies the AB site, the corresponding host-atom bond is significantly extended. We observe the same phenomenon in $\mathrm{In}_2\mathrm{O}_3$. This may explain why

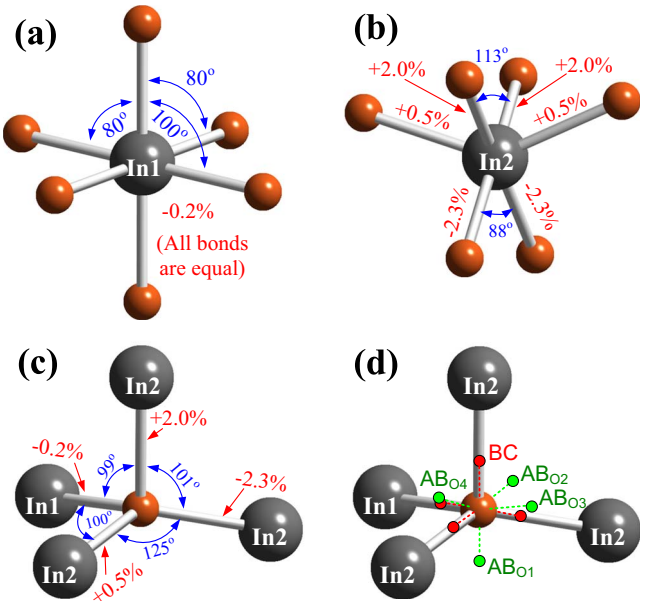

FIG. 1. (Color online) Schematic illustration of the coordination around In and O atoms in $\mathrm{In}_2\mathrm{O}_3$. The percentage numbers indicate the differences in bond length compared to the average of all In-O bonds (calculated value=2.169 Å). There are two In inequivalent sites, both surrounded by six O atoms. All O sites are equivalent and surrounded by four In atoms. (a) The $8b$ In site, (b) the $24d$ In site, (c) the O site, and (d) the possible sites for interstitial H.

TABLE I. Calculated formation energies E^f for H defects and O vacancies in $\mathrm{In}_2\mathrm{O}_3$. For some defects with an occupied gap state, a corrected value of E^f based on LDA+U and extrapolation (Ref. 19) (see text) is presented in square brackets. For charged defects we take the Fermi energy at the VBM. Equilibrium with bulk In metal (In-rich conditions) and with H_2 molecules at T=0 is assumed. Bond lengths for O-H bonds in the antibonding configurations of H_i^+ are also listed.

Defect	Location	E^f (eV)	$d_{\mathrm{O\text{-}H}}$ (Å)
H_i^+	$\mathrm{AB}_{\mathrm{O1}}$	−2.09	1.026
H_i^+	$\mathrm{AB}_{\mathrm{O2}}$	−1.66	1.015
H_i^+	$\mathrm{AB}_{\mathrm{O3}}$	−1.34	0.995
H_i^+	$\mathrm{AB}_{\mathrm{O4}}$	−1.35	0.996
H_i^0	$16c$	2.43	
H_i^-	$16c$	3.41 [4.27]	
H_i^-	$8a$	4.33	
$\mathrm{H}_{\mathrm{O}}^+$	O site	−1.40	
V_{O}^{2+}	O site	−2.68	
V_{O}^+	O site	−0.84[0.01]	
V_{O}^0	O site	0.96 [2.30]	

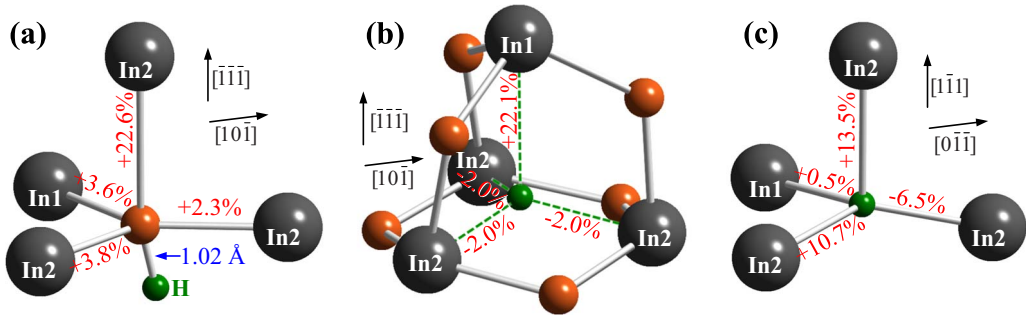

FIG. 2. (Color online) Schematic illustration of H defects in In_2O_3. H_i^+ at the AB_{O1} site in (a), H_i^- at the 16*c* site in (b), and H_O^+ in (c).

the AB_{O1} site is the preferred site for H_i^+, since its corresponding In-O bond is initially the longest. H_i^+ at the AB_{O1} site is lower in energy than the other (metastable) sites by at least 0.4 eV, rendering the occupation of those other sites negligible at reasonable temperatures. The fully relaxed geometry of H_i^+ at the AB_{O1} site is shown in Fig. 2(a). The O-H bond distances ($d_{O\text{-}H}$), as shown in Table I, are slightly longer than the O-H bond in H_2O. A similar trend was observed for the case of H_i in ZnO.[25]

In the negative charge state, H_i prefers interstitial sites closer to the cations.[20,23] In the bixbyite crystal, two such interstitial sites exist, which we will refer to as 8*a* and 16*c* following their Wyckoff notations.[15] We find that H_i^- and H_i^0 are stable at the 16*c* site with the single-electron level at ~1 eV above the valence-band maximum (VBM); the corresponding defect state is spatially localized on the H atom. The relaxed geometry of H_i^- at the 16*c* site is shown in Fig. 2(b). At the 8*a* site H_i^- is metastable with a formation energy that is higher by 0.9 eV than at the 16*c* site.

The formation energies for H_i^- and H_i^0 are shown in Table I, and a plot of formation energy as a function of Fermi-level position for all three charge states is shown in Fig. 3. Based on the LDA results, H_i is a negative-*U* defect (the neutral charge state is never stable). H_i is stable in the + charge state for the range of Fermi energies from the VBM up to E_F ~2.75 eV above the VBM. Since the band gap of MBE-grown In_2O_3 has been reported to be 2.67 eV,[17] we can conclude that hydrogen behaves exclusively as a donor for Fermi levels within this gap.

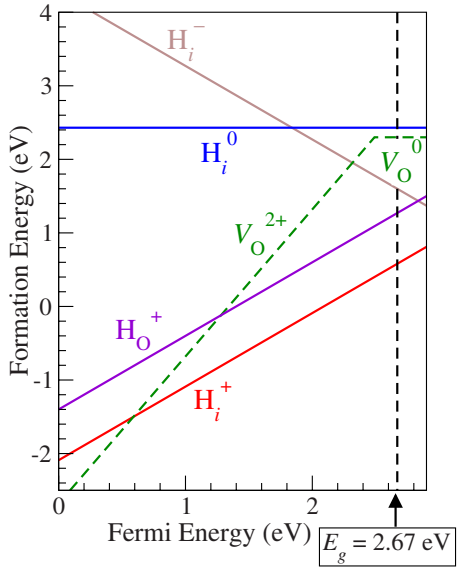

FIG. 3. (Color online) Calculated formation energies of hydrogen defects and oxygen vacancies in In_2O_3 as a function of Fermi energy. In-rich conditions are assumed.

The bare LDA results show that the +/− transition level (the Fermi-level value for which H_i^+ and H_i^- have equal formation energies) occurs at 2.75 eV above the VBM. Since this value is only slightly above the reported gap of 2.67 eV,[17] and since there may still be some uncertainty in this band-gap value (due to the band-gap renormalization and the potential residual strain in the thin films), it is worthwhile to obtain a more reliable value for the +/− transition level by going beyond the bare LDA results. LDA underestimates the band gap and, therefore, also the energy of H_i^-, which has an occupied state in the band gap. Correction of the band gap may shift this state upward and hence increase the energy of H_i^-. To estimate this correction, we performed LDA+*U* calculations as described in Ref. 19 with U=4 eV for the In 4*d* states. The LDA+*U* calculation for bulk In_2O_3 produces a slightly reduced lattice constant (by 1.4%) and raises the band gap by 0.47 eV compared to LDA. To obtain a complete band-gap correction, further extrapolation is needed.[19] Based on the calculations of bulk band gap, we can see that the correction has to be scaled up by $(2.67-1.17)/0.47=3.19$ times to get the full band-gap correction. The LDA+*U* calculations of H_i^- raise the +/− level by 0.14 eV; therefore, the corrected transition level would occur at $2.75+0.14\times3.19=3.20$ eV, which is well above the conduction-band minimum (CBM). The corrected formation energy of H_i^- is shown in Fig. 3.

In addition to H_i, we have studied H substitution on the O site, finding that H_O is also exclusively a donor. It always exists in + charge state without any defect level inside the band gap. The fully relaxed geometry of H_O^+ is shown in Fig. 2(c), and the calculated formation energy of H_O is included in Table I and plotted in Fig. 3. The formation energy of H_O is slightly higher than that of H_i, but low enough to lead to a significant incorporation of substitutional hydrogen. We also performed calculations for oxygen vacancies in order to investigate the stability of H_O with respect to the dissociation into H_i and V_O. We find that V_O is a deep donor in In_2O_3. Our calculations show that V_O is stable in two charge states: 2+ and neutral; the + charge state is never stable. We again used the LDA+*U* extrapolation scheme; formation energies based on LDA and LDA+*U* are listed in Table I, and the corrected

formation energies are shown in Fig. 3. Our calculated 2+/0 level, referenced to the VBM, is in good agreement with that calculated by Lany and Zunger.[26] (Note that in Lany and Zunger's work, the transition level for V_O appears to be much deeper in the gap because they used a larger In_2O_3 bandgap of 3.50 eV.) The binding energy between V_O and H_i to form H_O can be calculated from the formation energies of the three defects, shown in Fig. 3. Under *n*-type conditions the binding energy is 1.82 eV, a large value which is indicative of the stability of the substitutional hydrogen.

Recently, Koida *et al.*[1] prepared and characterized rf magnetron sputtered In_2O_3 samples doped with various concentrations of hydrogen. They reported an optimized carrier density of 3×10^{20} cm^{-3} and mobility as high as 130 $cm^2/V\,s$ for a sample doped with ~3 at. % of H. King *et al.*[27] performed muon spin rotation measurements to investigate the electrical behavior of hydrogen in In_2O_3. Their results indicate that hydrogen is a shallow donor, with the estimated +/− transition level at 0.6 eV above the conduction-band minimum.[27] These experimental results are consistent with our calculations, which indicate that both interstitial and substitutional hydrogen serve as donors in In_2O_3.

S.L. and P.R. thank the Thailand Research Fund (Grants No. RTA5280009 and No. PHD/0203/2546) and AOARD/AFOSR (Contract No. FA2386-09-1-4106). The work in the US was supported in part by the MRSEC Program of the National Science Foundation under Award No. DMR05-20415, by the NSF IMI Program under Award No. DMR 04-09848, and by the UCSB Solid State Lighting and Display Center. This work also made use of the CNSI Computing Facility under NSF Grant No. CHE-0321368.

[1] T. Koida, H. Fujiwara, and M. Kondo, Jpn. J. Appl. Phys. **46**, L685 (2007).
[2] C. G. Van de Walle, Phys. Rev. Lett. **85**, 1012 (2000).
[3] D. M. Hofmann, A. Hofstaetter, F. Leiter, H. Zhou, F. Henecker, B. K. Meyer, S. B. Orlinskii, J. Schmidt, and P. G. Baranov, Phys. Rev. Lett. **88**, 045504 (2002).
[4] A. Janotti and C. G. Van de Walle, Nature Mater. **6**, 44 (2007).
[5] A. Janotti and C. G. Van de Walle, Appl. Phys. Lett. **92**, 032104 (2008).
[6] A. K. Singh, A. Janotti, M. Scheffler, and C. G. Van de Walle, Phys. Rev. Lett. **101**, 055502 (2008).
[7] H. Odaka, S. Iwata, N. Taga, S. Ohnishi, Y. Kaneta, and Y. Shigesato, Jpn. J. Appl. Phys. **36**, 5551 (1997).
[8] O. N. Mryasov and A. J. Freeman, Phys. Rev. B **64**, 233111 (2001).
[9] J. E. Medvedeva, Phys. Rev. Lett. **97**, 086401 (2006).
[10] H. Odaka, Y. Shigesato, T. Murakami, and S. Iwata, Jpn. J. Appl. Phys. **40**, 3231 (2001).
[11] O. Warschkow, D. E. Ellis, G. B. Gonzalez, and T. O. Mason, J. Am. Ceram. Soc. **86**, 1700 (2003).
[12] G. Kresse and J. Furthmüller, Comput. Mater. Sci. **6**, 15 (1996).
[13] P. E. Blöchl, Phys. Rev. B **50**, 17953 (1994).
[14] H. J. Monkhorst and J. D. Pack, Phys. Rev. B **13**, 5188 (1976).
[15] M. Marezio, Acta Crystallogr. **20**, 723 (1966).
[16] A. Klein, Appl. Phys. Lett. **77**, 2009 (2000).
[17] A. Bourlange, D. J. Payne, R. G. Egdell, J. S. Foord, P. P. Edwards, M. O. Jones, A. Schertel, P. J. Dobson, and J. L. Hutchison, Appl. Phys. Lett. **92**, 092117 (2008).
[18] A. Walsh, J. L. F. Da Silva, S.-H. Wei, C. Korber, A. Klein, L. F. J. Piper, A. DeMasi, K. E. Smith, G. Panaccione, P. Torelli, D. J. Payne, A. Bourlange, and R. G. Egdell, Phys. Rev. Lett. **100**, 167402 (2008).
[19] A. Janotti and C. G. Van de Walle, Phys. Rev. B **76**, 165202 (2007).
[20] S. Limpijumnong and C. G. Van de Walle, Phys. Status Solidi B **228**, 303 (2001).
[21] C. G. Van de Walle, S. Limpijumnong, and J. Neugebauer, Phys. Rev. B **63**, 245205 (2001).
[22] S. Limpijumnong and S. B. Zhang, Appl. Phys. Lett. **86**, 151910 (2005).
[23] S. Limpijumnong, J. E. Northrup, and C. G. Van de Walle, Phys. Rev. B **68**, 075206 (2003).
[24] S. Limpijumnong, J. E. Northrup, and C. G. Van de Walle, Phys. Rev. Lett. **87**, 205505 (2001).
[25] S. Limpijumnong, *Hydrogen in Semiconductors*, edited by N. H. Nickel. M. D. McCluskey, and S. B. Zhang, MRS Symposia Proceedings No. 813 (Materials Research Society, Pittsburg, 2004) p. H3.6.1.
[26] S. Lany and A. Zunger, Phys. Rev. Lett. **98**, 045501 (2007).
[27] P. D. C. King, R. L. Lichti, Y. G. Celebi, J. M. Gil, R. C. Vilao, H. V. Alberto, J. Piroto Duarte, D. J. Payne, R. G. Egdell, I. McKenzie, C. F. McConville, S. F. J. Cox, and T. D. Veal, Phys. Rev. B **80**, 081201(R) (2009).